

Localization of strain and the melting wave in high-speed penetration

M.V. Ayzenberg–Stepanenko¹ and L.I. Slepyan²

¹*Department of Mathematics, Ben Gurion University, Beer-Sheva 84105 Israel*

²*Department of Solid Mechanics, Materials and Systems
Tel Aviv University, Ramat Aviv 69978 Israel*

Abstract. Localization of shear under high-speed penetration is shown to be accompanied by initiation of a melting wave. Transient, self-similar and steady-state problems of heating and melting of the material under idealized conditions of penetration are studied, and the role of plastic hardening is examined. A critical value of the discontinuity in the velocity in the shear bend is found: the melting wave arises independently of the hardening modulus if the discontinuity exceeds this point. Resistance to shear in the melting wave is shown to decrease drastically. This ensures the separation of the flow jets from the surrounding material. Thus, the plastic jet model of penetration is justified.

1 Introduction

1.1 Hydrodynamic models of penetration

Well-known hydrodynamic models of penetration have a half-century history and take their origin from the work of Birkhoff *et al.* (1948), where penetration is considered as a collision of two jets of ideal fluids. In this model, the penetration velocity follows immediately from the Bernoulli equation. Allen and Rogers (1961) and then Alekseevskii (1966) and Tate (1967) introduced into this equation the so-called flow strength parameters to take into account the strength of the projectile and target materials. A comprehensive historical review and analysis of potentialities of these models, their advantages and drawbacks can be found in Zukas (1990).

D.Durban and J.R.A. Pearson (eds),

IUTAM Symposium on Non-Linear Singularities in Deformation and Flow, 129-140.

Kluwer Academic Publishers. Printed in the Netherlands.

Such a model permits the penetration depth and the projectile erosion to be determined. At the same time, it provides no way for determining the crater geometry and the mushrooming radius of the projectile. In this connection, a version of the hydrodynamic model has been elaborated by Slepyan (1978) for describing the movement of a rigid projectile or an ideal fluid jet in a deformable medium. The flow of the materials is assumed to exist only within an area of a finite, current radius, which is determined together with the other parameters of the process based on a given strength parameter of the target and the current velocity of the penetration. The surrounding material is assumed to be at rest.

This model can be used for an estimation of the resistance to the movement, the mushrooming radius of the projectile (for the fluid jet), and the size of the crater created. However, in the case of plastic materials such a hydrodynamic model cannot be used immediately. First, this model does not take into account energy loss in plastic deformation of the backward jets. Second, the conditions which allow interaction between the ideal jets and the surrounding immobile material to be neglected have not been established.

In the present paper, the latter problem is considered. It is shown that for high-speed penetration, localization of shear as a discontinuity in the flow of the material leads to initiation of a melting wave. Resistance to shear in the melting wave drastically decreases, and this results in separation of the flow jets and the surrounding, immobile material with negligible shear stresses in the interface. This allows the plastic jet model to be justified.

As to the energy loss in the backward jets, we only note here that the plastic work can be determined based on the scheme of proportional strain of the materials, which allows this work to be defined in terms of the initial and final parameters of the flow present in the hydrodynamic model formulation. This leads to the modified Bernoulli equation valid for plastic jets, and finally, to the closed system of governing equations.

1.2 Localization of shear

As is known, instability of a uniform plastic strain can arise under dynamic shear and this manifests itself in shear bands in thermoplastic solids (Recht, 1964; Anand *et al.*, 1986; Barta, 1987; Molinary and Clifton, 1987; Wright and Walter, 1987, 1996; Meunier *et al.*, 1992; Bai and Dodd, 1992; Gioia and Ortiz, 1996). Scores of works are devoted to measurement and description of initiation and propagation of the localized shear bands under various conditions. In such a band, local temperature is shown to rise by several hundred degrees (Hartley, 1987; Marchard and Duffy, 1988; Zehnder and Kallivayalil, 1991; Bai and Dodd, 1992; Zender and Rosakis, 1992a,b; Zhou *et al.*, 1996a,b). It can increase with the rate and duration of the shear, and under certain conditions this may lead

to melting of the material (Marchard and Duffy, 1988; Nicolas and Rajendran, 1990; Zhou *et al.*, 1996a). Our goal is to derive an estimation of (a) the conditions which give rise to the melting, and (b) the resistance to shear in the melting wave.

A theoretical treatment of the process of strain localization with initiation of a melting wave requires knowledge of the dependence of stresses on the high-level strain, strain rate and temperature. As far as we know, there are no sufficient data concerning such a dependence, and the considerations below are necessarily based on an idealized formulation. In particular, a linear hardening is assumed. However, it is shown that a critical value of the jump in velocity in the shear bend does exist: the melting wave arises independently of the hardening modulus if the jump exceeds this point.

2 Temperature in the localized shear band

To justify the acceptability of a corresponding idealized formulation, we begin with the analysis of the role of strain hardening in heating of the material by dynamic plastic shear.

First of all let us introduce parameters of the material used in calculations and estimations:

- density $\rho = 8 \cdot 10^3 \text{ kg/m}^3$,
- critical shear stress (equal to half the yielding limit) $\tau_0 = 2.5 \cdot 10^8 \text{ N/m}^2$,
- hardening modulus k which varies in the calculations,
- coefficient of viscosity $\mu = 10^{-2} \text{ Ns/m}^2$,
- heat capacity $c = 5 \cdot 10^2 \text{ Nm/(kg } ^\circ\text{K)}$,
- heat conductivity $\lambda = 50 \text{ N/(s } ^\circ\text{K)}$,
- melting point $\Theta = 1.8 \cdot 10^3 \text{ } ^\circ\text{K}$ and
- latent heat of melting $L = 2.5 \cdot 10^5 \text{ Nm/kg}$.

Using these constants the natural units are introduced as

- length-unit $l_0 = 2\sqrt{\lambda\mu/(\rho c\tau_0)} \approx 4 \cdot 10^{-8} \text{ m}$
- time-unit $t_0 = \mu/\tau_0 = 4 \cdot 10^{-11} \text{ s}$, the corresponding
- speed-unit $d_0 = 10^3 \text{ m/s}$ and
- temperature-unit $\theta_0 = \tau_0/(\rho c) = 62.5 \text{ } ^\circ\text{K}$.

2.1 One-dimensional transient problem of heating

In our problem, heating and melting of the material are induced by a given, tangential particle velocity, v_0 , at the boundary of a half-space of a thermoplastic material and the propagation velocity of this external action, b . These velocities are assumed to correspond to the above-mentioned jump in velocity in the shear bend and its propagation during the penetration.

Consider a half-space, $x > 0$, of a rigid-plastic material under antiplane dynamic shear and under the following conditions. Shear stresses are assumed to correspond to a linear hardening:

$$\tau = \tau_0 \operatorname{sign} \frac{\partial w(x, t)}{\partial x} + k \frac{\partial w(x, t)}{\partial x}, \quad (1)$$

where w denotes displacements directed along a normal to x ; τ_0 and k are positive constants. In the considered uncoupled problem, where τ_0 and k are assumed to be independent of temperature, the dynamic equation of motion is the one-dimensional wave equation:

$$\frac{\partial^2 w(x, t)}{\partial t^2} - a^2 \frac{\partial^2 w(x, t)}{\partial x^2} = 0, \quad a^2 = \frac{k}{\rho}, \quad (2)$$

where a is the wave speed.

It is assumed that the work of plastic strain transfers into heat totally, that is, a small part of such work going into energy of micro-strain is neglected. Taking the work of plastic strain into account, the Fourier equation is assumed to govern heat conductivity over the half-space as

$$\rho c \frac{\partial \theta(x, t)}{\partial t} - \lambda \frac{\partial^2 \theta(x, t)}{\partial x^2} = \frac{\partial U(x, t)}{\partial t}, \quad (3)$$

where U is the plastic strain energy density per unit volume.

The initial and boundary conditions are as follows:

$$\begin{aligned} w &= \frac{\partial w}{\partial t} = 0, \quad \theta = \theta_0 = \text{const} \quad (t = 0, x > 0) \\ v \equiv \frac{\partial w}{\partial t} &= v_0, \quad N = -\lambda \frac{\partial \theta}{\partial x} = 0 \quad (x = 0, t > 0). \end{aligned} \quad (4)$$

Here N is the heat flux. This formulation leads to the solution

$$\begin{aligned} U &= \frac{v_0}{a} \left(\tau_0 + \frac{kv_0}{2a} \right) \\ \theta &= \theta_0 + \left(\frac{\tau_0 v_0}{\rho c a} + \frac{v_0^2}{2c} \right) \left[1 - \exp(\alpha t) \operatorname{erfc}(\sqrt{\alpha t}) \right] \\ &= \theta_0 + \frac{1}{c} \left(\frac{\tau_0 v_0}{\sqrt{k\rho}} + \frac{v_0^2}{2} \right) \left[1 - \frac{2}{\pi} \int_0^\infty \frac{\exp(-\alpha t z^2)}{1 + z^2} dz \right], \end{aligned} \quad (5)$$

where $\alpha = \rho c a^2 / \lambda = kc / \lambda$ and

$$\operatorname{erfc}(y) = 1 - \operatorname{erf}(y) = \frac{2}{\sqrt{\pi}} \int_x^\infty \exp(-z^2) dz$$

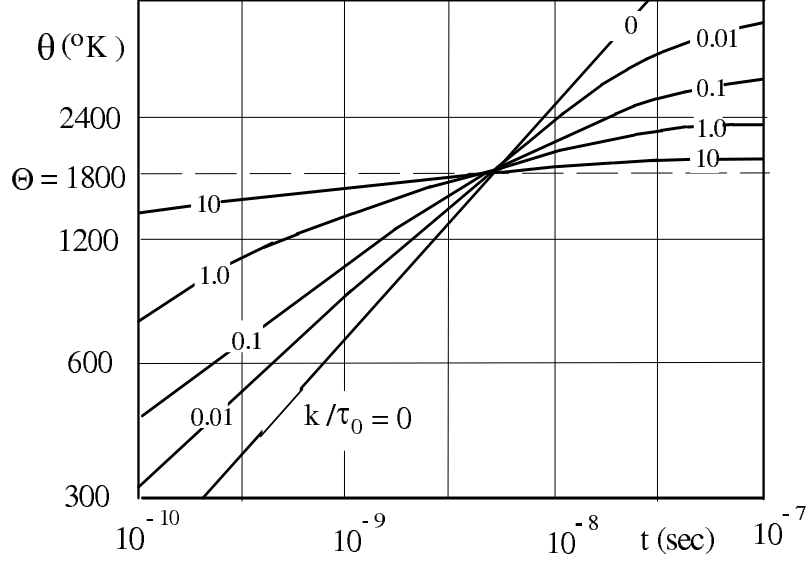


Figure 1: Temperature vs. time at $v_0 = 1250 \text{ m/s}$ and various hardening modules

It can be observed that temperature increases monotonically with time, as fast as α is large, and tends to the limit

$$\theta = \theta_0 + \frac{\tau_0 v_0}{\rho c a} + \frac{v_0^2}{2c} \quad (6)$$

if $k > 0$. Otherwise, if $k = 0$

$$\theta = \theta_0 + \frac{2\tau_0 v_0}{\sqrt{\pi \lambda \rho c}} \sqrt{t}. \quad (7)$$

These dependences are valid when the temperature is under the melting point (and if it does not influence the resistance to plastic strain as assumed). The main question is whether the temperature achieves the melting point and how long the corresponding time of heating is. As follows from these results, the limiting temperature increases with decrease in hardening, and the limiting velocity, v_0 , required for the temperature to achieve the melting point decreases together with hardening. The critical value v_* of the velocity v_0 is found such that provides temperature of the melting point independently of hardening. Under the above-mentioned parameters, $v_* = 1225 \text{ m/s}$ (for the initial temperature $\theta_0 = 300^\circ \text{K}$). If v_0 exceeds v_* only a little, the temperature achieves the melting point very soon, and it does not matter what hardening of the material is. The characteristic time is of the order of $4 \cdot 10^{-9} \text{ s}$. In the Fig. 1, dependencies of the temperature on time are plotted at $v_0 = 1250 \text{ m/s}$.

2.2 Steady-state, 2D problem of heating

Consider a space, x, y, z , filled by the rigid-plastic material (1), the same as above, under the condition at the interface $x = 0$:

$$\frac{\partial w}{\partial t} = \pm v_0 H(\eta) \quad (x = \pm 0), \quad \eta = bt - y. \quad (8)$$

This action is assumed to induce plastic waves propagating with a velocity $a < b$. The formulation leads to the solution

$$\theta = \theta_0 + \frac{2\tau_0 v_0}{\pi \rho c b} \left[1 + \nu \int_0^\eta K_0(\nu \eta) \exp(\nu \eta) d\eta \right], \quad (9)$$

where the Bessel function, K_0 , and the parameter ν are defined by the relations

$$K_0(x) = \int_1^\infty \frac{\exp(-xt)}{\sqrt{t^2 - 1}} dt, \quad \nu = \frac{\rho c b}{2\lambda} = 4 \cdot 10^7 \text{ 1/m}. \quad (10)$$

Note that for large $\nu \eta$

$$\theta - \theta_0 \sim \frac{2\tau_0 v_0}{\sqrt{\pi \lambda \rho b c}} \sqrt{\eta}. \quad (11)$$

This result completely corresponds to the above-considered one-dimensional problem (7).

It can be seen that for the high-speed penetration (when $b \approx 1,000 \text{ m/s}$ or higher), the distance η where the asymptote (11) is valid is very small [see (9) and expression (10) for ν]. Thus the 1D formulation of the problem is acceptable here.

3 Melting wave

3.1 One-dimensional melting wave

Thus the 2D temperature field produced by the shear action, propagating with the velocity b of the order of 1,000 m/s, approaches closely the 1D field very soon (at a very small distance from the front of the action, $y = bt$). The same conclusion is valid for the melting wave considered below, because the equations for viscous fluid dynamics (dynamics of the melt-down material) and for heat conductivity are of the same type and, as is shown below, the wave of particle velocities propagates even slower than the temperature wave. This allows restriction by the 1D formulation for the melting wave. Note that it is common for the description of a viscous boundary layer.

Also, as was shown, the temperature achieves the melting point very soon for any hardening if the velocity, v_0 , exceeds the critical value v_* . This necessarily

results in localization of strain, and this allows, for describing the melting wave, an idealized rigid-plastic material without hardening to be considered.

With the goal to describe the corresponding melting wave and to find the distributions of temperature and shear stresses in such a wave, consider the antiplane problem for a visco-plastic material described below. The same coordinates are used as in the above-considered 1D problem of heating. So, the particle velocities $v = v_z$ and temperature are assumed to depend on the coordinate x and time t .

The material is assumed to be a rigid-plastic solid if temperature $\theta < \Theta$, where Θ is the melting point, and it is a viscous liquid if $\theta > \Theta$. The latent heat of melting, L , is required to melt it down. The limiting shear stresses in the material are τ_0 for both the solid and liquid states. In the solid state, there is no strain rate if the stress $\tau = \tau_{xz} < \tau_0$, and slip can exist in the plane and in the direction of the maximal stress if $\tau = \tau_0$. In the liquid state

$$\tau = \mu \frac{\partial v}{\partial x}, \quad 0 \leq v \leq v_+ \leq v_0, \quad (12)$$

with a continuous velocity: $v_+ = v_0$ (v_+ is the limit of v at the boundary from the right) if $\tau < \tau_0$ or $v_+ \leq v_0$ if $\tau = \tau_0$.

The flow of the material is represented consisting of two regions separated by a moving interface. In the first region the material is melt down, it is considered as a viscous fluid, and the material is rigid in the second region. The temperature at the interface is equal to the melting point, Θ . At the interface as the melting wavefront, there is an energy release equal to the latent heat of melting, L . This energy release is provided by a jump in heat flux, namely,

$$N_- - N_+ = \rho L W \quad (13)$$

where N_+ and N_- are the heat fluxes in front of and behind the moving interface, respectively, and W is its speed (the speed of the wavefront). At the same time, the particle velocity, v (in z -direction) is assumed to be continuous at the moving interface. The temperature at the interface is continuous too.

The process can be divided into three periods. In the first, $0 < t < t_1$, temperature $\theta < \Theta$, and $v = 0$. A growing layer of the melt-down material arises at $t = t_1$. However, in the second period, $t_1 < t < t_2$, the velocity of the material at $x = 0$ does not achieve the applied velocity v_0 ($v_+ < v_0$). At last, in the third period ($t > t_2$), $v_+ = v_0$.

Thus consider the half-space, $x > 0$, filled by a plastic material which is initially at rest. Under a given particle velocity, v_0 , at the boundary, $x = 0$, the melting wave is expected to arise in the increasing region, $0 < x < X(t)$, $dX/dt \geq 0$, where the material becomes a viscous liquid. The equation of motion is valid as

$$\rho \frac{\partial v}{\partial t} = \frac{\partial \tau}{\partial x}, \quad (14)$$

where $v(0, t) = v_+$. Under the linear viscosity relationship (12), where $\mu = \text{const}$ (a dependence of μ on temperature is neglected), the velocity obeys the equation

$$\rho \frac{\partial v}{\partial t} = \mu \frac{\partial^2 v}{\partial x^2} \quad (15)$$

in the region $0 < x < X$, where $\theta > \Theta$, and the material is at rest for $x > X(t)$.

The Fourier equation is assumed to govern heat transfer over the half-space, $0 < x < \infty$:

$$\rho c \frac{\partial \theta}{\partial t} - \lambda \frac{\partial^2 \theta}{\partial x^2} = \tau \frac{\partial v}{\partial x} = \mu \left(\frac{\partial v}{\partial x} \right)^2, \quad (16)$$

where c and λ are specific heat capacity and thermo-conductivity, accordingly. These coefficients are considered to be constant as well as μ . The right hand part of this equation corresponds to the heat production by the work of shear viscosity stresses in the region $0 < x < X(t)$. The following additional conditions are imposed:

the stress or the velocity at $x = 0$:

$$\tau = \tau_0 \quad [v(0, t) = v_+ < v_0] \quad \text{or} \quad v(0, t) = v_0 \quad [\tau(0, t) < \tau_0], \quad (17)$$

the velocity at $x = X$:

$$v(X, t) = 0, \quad (18)$$

the heat flow through the boundary, $x = 0$, if $v_+ < v_0$; otherwise, there is no heat flow at $x = 0$:

$$-\lambda \frac{\partial \theta}{\partial x} = \tau_0 (v_0 - v_+) H(v_0 - v_+) \quad (x = 0), \quad (19)$$

temperature at the moving interface

$$\theta = \Theta \quad [x = X(t)], \quad (20)$$

continuity of temperature at $x = X$:

$$[\theta] = 0 \quad (x = X), \quad (21)$$

temperature at infinity

$$\theta = 0 \quad (x = \infty). \quad (22)$$

Thus, for the determination of solutions to these two equations, each of the second order (one of them is defined in one region, and the other is for two regions) and the coordinate of the wavefront, $X(t)$, there are seven conditions: Eqs. (17) – (22) and the energy-release-rate relation (13):

$$\lambda \left(\frac{\partial \theta(X+0, t)}{\partial x} - \frac{\partial \theta(X-0, t)}{\partial x} \right) = \rho L \frac{dX}{dt}. \quad (23)$$

It could be shown that in the third period the fields of stresses and temperature tend to the corresponding fields for the related self-similar solution. Taking into account the first and second periods turn out to be very short, it can be said that such a self-similar solution gives us an adequate representation of the melting wave.

3.2 Self-similar solution for the melting wave

In the case when the constitutive equation for the melt-down material (12) is assumed to be valid independently of the level of stresses, the self-similar solution exists which satisfies all the equations and additional conditions

$$v = v(\eta), \quad \theta = \theta(\eta), \quad \eta = \frac{\rho x^2}{4\mu t}, \quad t > 0, \quad (24)$$

In these terms, stresses, the governing equations and the additional conditions take the form

$$\tau = \sqrt{\frac{\mu\rho\eta}{t}} v' \quad \left(v' = \frac{dv}{d\eta} \right), \quad (25)$$

$$v'' + \left(1 + \frac{1}{2\eta} \right) v' = 0 \quad (26)$$

$$\theta'' + \left(\kappa + \frac{1}{2\eta} \right) \theta' = -\frac{\mu}{\lambda} (v')^2, \quad \kappa = \frac{c\mu}{\lambda}. \quad (27)$$

Further

$$v = v_0 \quad (\eta = 0), \quad v = 0 \quad (\eta = Y), \quad (28)$$

where the point $\eta = Y$ corresponds to the wavefront (in the self-similar solution considered, $X(t) = 2\sqrt{\mu Y t / \rho}$),

$$\zeta = \sqrt{\eta} \theta' \rightarrow 0 \quad (\eta \rightarrow 0), \quad (29)$$

$$N_- - N_+ = \lambda(\zeta_+ - \zeta_-) \sqrt{\frac{\rho}{\mu t}} = \rho L \sqrt{\frac{\mu Y}{\rho t}} \quad (\eta = Y), \quad (30)$$

$$\theta = \Theta \quad (\eta = Y), \quad \theta = 0 \quad (\eta = \infty). \quad (31)$$

Equation (26), with conditions (28), leads to the solution

$$v = v_0 \left[1 - \frac{\operatorname{erf}(\sqrt{\eta})}{\operatorname{erf}(\sqrt{Y})} \right] \quad (32)$$

Equation (27) can be represented in the form

$$\zeta' + \kappa \zeta = -\frac{\mu}{\lambda} (v')^2 \sqrt{\eta} = -\frac{v_0^2 \mu \exp(-2\eta)}{\pi \lambda \sqrt{\eta} \operatorname{erf}^2(\sqrt{Y})} H(Y - \eta). \quad (33)$$

This equation, with conditions (29) and (31), gives us the solution

$$\zeta = -\frac{v_0^2 \mu}{\lambda \sqrt{2\pi(2-\kappa)}} \frac{\operatorname{erf}[\sqrt{(2-\kappa)\eta}]}{\operatorname{erf}^2(\sqrt{Y})} e^{-\kappa\eta} \quad (\eta < Y)$$

$$\zeta = -\frac{\Theta \sqrt{Y} \exp(-\kappa\eta)}{\sqrt{\pi} \operatorname{erfc}(\sqrt{\kappa Y})} \quad (\eta > Y) \quad (34)$$

and the temperature field under condition (31)

$$\theta = \Theta + \frac{v_0^2 \mu}{\lambda \sqrt{2\pi(2-\kappa)} \operatorname{erf}^2(\sqrt{Y})} I \quad (\eta < Y)$$

$$I = \int_{\eta}^Y \operatorname{erf}\left(\sqrt{(2-\kappa)\eta}\right) e^{-\kappa\eta} \frac{d\eta}{\sqrt{\eta}}$$

$$\theta = \Theta \frac{\operatorname{erfc}(\sqrt{\kappa\eta})}{\operatorname{erfc}(\sqrt{\kappa Y})} \quad (\eta > Y). \quad (35)$$

The rest of condition (30) gives us an equation with respect to the wave front coordinate Y

$$\frac{v_0^2}{\sqrt{2\pi(2-\kappa)Y}} \frac{\operatorname{erf}(\sqrt{(2-\kappa)Y})}{\operatorname{erf}^2(\sqrt{Y})} - \frac{\Theta \lambda}{\sqrt{\pi} \mu \operatorname{erfc}(\sqrt{\kappa Y})} = L e^{\kappa Y}. \quad (36)$$

Consider two asymptotic cases. The low-velocity case, when $v_0 \rightarrow 0$, corresponds to the vanishing of the melt-down-material zone: $Y \rightarrow 0$. In this case, it follows from (36) that

$$Y \sim \frac{\sqrt{\pi} \mu v_0^2}{2\sqrt{2}(\Theta \lambda + \sqrt{\pi} \mu L)} \approx 8 \cdot 10^{-8} v_0^2 \quad (v_0 \rightarrow 0), \quad (37)$$

and at $\eta < Y$:

$$v \sim v_0 \left(1 - \sqrt{\frac{\eta}{Y}}\right), \quad (38)$$

$$\tau \sim -\frac{v_0}{2} \sqrt{\frac{\rho \mu}{Y t}} \approx -\frac{6 \cdot 10^{-5}}{\sqrt{t}}, \quad (39)$$

$$\theta \sim \Theta. \quad (40)$$

The high-velocity case ($v_0 \rightarrow \infty$) corresponds to $Y \rightarrow \infty$. In this case, it can be found that

$$Y = Y_1 - Y_2 + o(1), \quad (41)$$

where

$$Y_1 = \ln A - \frac{1}{\kappa} \ln \ln A, \quad A = \left[\frac{\mu v_0^2}{\Theta \lambda \sqrt{2\pi\kappa(2-\kappa)}} \right]^{1/\kappa}, \quad (42)$$

$$Y_2 = \frac{1}{\kappa} \ln \left[1 + \sqrt{2\pi(2-\kappa)} Y_1 \frac{L}{v_0^2} \exp(\kappa Y_1) \right], \quad (43)$$

and at $\eta < Y$:

$$v \sim v_0 [1 - \operatorname{erf}(\eta)], \quad (44)$$

$$\tau \sim -v_0 \sqrt{\frac{\rho\mu}{\pi t}} e^{-\eta} \approx -\frac{1.8v_0}{\sqrt{t}} e^{-\eta}, \quad (45)$$

$$\theta \sim \Theta + \frac{v_0^2 \mu}{\lambda \sqrt{2\pi(2-\kappa)}} \int_{\eta}^{\infty} \operatorname{erf}(\sqrt{(2-\kappa)\eta}) e^{-\kappa\eta} \frac{d\eta}{\sqrt{\eta}}. \quad (46)$$

It can be seen that the velocity, v_0 , of the order of 10^3 m/s corresponds to the low-velocity case ($Y \approx 0.08$). In this case, the shear stresses comprise only 6% of the yield limit τ_0 when $t \geq 10^{-6}$ s. As follows from (45), τ increases with the velocity, however, the ratio $\tau/(\rho v_0^2)$ decreases.

In applying these results to the projectile – target interaction, we assume that the moment $t = 0$ corresponds to the beginning of the plastic flow at a considered *material* coordinate. Thus, the distance from this initial point can be measured from the front point of the projectile. This distance can be expressed as $h = v_0 t$. Using the above-mentioned numerical values, it can be found that the shear stresses fall drastically at the distance of the order of $10^3 \cdot 10^{-6} = 10^{-3}$ m. Thus, for a projectile of the length of several cm, the shear resistance in the localized shear bend can really be neglected.

4 Acknowledgment

This research was supported by grant No. 94-00349 from the United States – Israel Binational Science Foundation (BSF), Jerusalem, Israel, and by grant No. 9673-1-96 from the Ministry of Science, Israel.

References

- [1] Alekseevskii, V. P. (1966) Penetration of a rod into a target at high velocity. *Combust., Explos., Shock Waves* **2**, 63-66.
- [2] Allen, W. A. and Rogers, J. W. (1961) Penetration of a rod into a semi-infinite target. *J. Franklin Inst.* **272**, 275-275.

- [3] Anand, L., Kim, K. H. and Shawki, T. G. (1986) Onset of shear localization in viscoplastic solids. *J. Mech. Phys. Solids* **35**, 407-429.
- [4] Bai, Y. and Dodd, B. (1992) *Adiabatic Shear Localization*. Pergamon. Oxford.
- [5] Barta, R. C. (1987) Effect of material parameters on the initiation and growth of adiabatic shear bands. *Int. J. Solid Struct.* **23**, 1435-1446.
- [6] Birkhoff, G., MacDougall, D. P., Pugh, E. M. and Taylor, G. I. (1948) Explosives with lined cavities. *J. Appl. Phys.* **19**, 563-582.
- [7] Gioia, G. and Ortiz, M. (1996) The two-dimensional structure of dynamic boundary layers and shear bands in thermoviscoplastic solids. *J. Mech. Phys. Solids* **44**, 251-292.
- [8] Hartley, K. A., Duffy, J. and Hawley, R.H. (1987) Measurement of the temperature profile during shear band formation in steels deforming at high strain rates. *J. Mech. Phys. Solids* **35**, 283-301.
- [9] Marchand, A. and Duffy, J. (1988) An experimental study of the formation process of adiabatic shear bands in a structural steel. *J. Mech. Phys. Solids* **36**, 251-283.
- [10] Meunier, Y., Roux, R. and Moureaud, J. (1992) Survey of adiabatic shear phenomena in armor steels with perforation. *Shock-Wave and High-Strain-Rate Phenomena in Materials* (ed. M. A. Meyers, L. E. Murr and K. P. Staudhammer), Marcel Dekker Inc., New-York, Basel, Hong Kong, 637-644.
- [11] Molinari, A. and Clifton, R. J. (1987) Analytical characterization of shear localization in thermoviscoplastic materials. *J. Appl. Mech., Trans. ASME* **54**, 806-812.
- [12] Nicolas T. and Rajendran, A. M. (1992) Material characterization at high strain rates. In: *High Velocity Impact Dynamics* (ed. Jonas A. Zukas), John Wiley & Sons, New York, 127-296.
- [13] Recht, R. F. (1964) Catastrophic thermoplastic shear. *J. Appl. Mech., Trans. ASME* **31E**, 189-193.
- [14] Slepyan, L. I. (1978) Calculation of the size of the crater formed by a high-speed impact. *Sov. Mining Sci.* **14**, 467-471.
- [15] Tate, A. (1967) A theory for the deceleration of long rods after impact. *J. Mech. Phys. Solids* **15**, 387-399.

- [16] Wright, T. W. and Walter, J.W. (1987) On stress collapse in adiabatic shear bands. *J. Mech. Phys. Solids* **35**, 701-720.
- [17] Wright, T. W. and Walter, J. W. (1996), The asymptotic structure of an adiabatic shear band in antiplane motion. *J. Mech. Phys. Solids* **44**, 77-97.
- [18] Zehnder, A. T. and Kallivayalil, J. A. (1991) Temperature rise due to dynamic crack growth in beta-C titanium. *Speckle Techniques, Birefringence Methods, and Applications to Solid Mechanics, SPIE* **1554A**, 48.
- [19] Zehnder, A. T. and Rosakis, A. J. (1992a) On the temperature distribution at the vicinity of dynamically propagating cracks in 4340 steel. *J. Mech. Phys. Solids* **39**, 385-415.
- [20] Zehnder, A. T. and Rosakis, A. J. (1992b) Temperature rise at the tip of dynamically propagating cracks: measurements using high-speed infrared detectors. *Experimental Techniques in Fracture* (ed. J. S. Epstein), VCH Publishers, 125-169.
- [21] Zhou, M., Rosakis, A. J., and Ravichandran, G. (1996a) Dynamically propagating shear bands in impact-loaded prenotched plates – I. Experimental investigations of temperature signatures and propagation speed. *J. Mech. Phys. Solids* **44**, 981-1006.
- [22] Zhou, M., Rosakis, A. J. and Ravichandran, G. (1996b) Dynamically propagating shear bands in impact-loaded prenotched plates – II. Numerical simulation. *J. Mech. Phys. Solids* **44**, 1007-1032.
- [23] Zukas, J. A. (ed.) (1990) *High Velocity Impact Dynamics*. John Wiley & Sons. New York.